# Subband Coded Image Reconstruction for Lossy Packet Networks

Sheila S. Hemami and Robert M. Gray

Information Systems Laboratory, Stanford University, CA 94305-4055

## Abstract

*Packet-based transmission of subband coded images over lossy networks presents a reconstruction problem at the decoder. This paper presents two techniques for reconstruction of lost subband coefficients. The low frequency reconstruction algorithm maintains smoothness and exploits intraband correlation by fitting a surface to known coefficients to interpolate lost coefficients. Accurate edge placement is achieved by warping the interpolation grid based on local high frequency characteristics. High frequency reconstruction is performed using linear interpolation, providing good visual performance and maintaining properties required for edge placement. The algorithm is applicable to any number of decompositions, both luminance and chrominance components, and can be used with progressive transmission. Computational overhead is minimal at 0.5% per percentage of coefficients lost and the reconstructed synthesized images maintain good visual quality at loss rates as high as 10%.*

## 1. Introduction

Packet-based transmission of digitally coded still images over lossy networks presents a reconstruction problem at the decoder. Standard techniques that work well for pure data, such as forward error correction (FEC) or automatic retransmission query protocols (ARQ) become unwieldy when applied to image and video signals. FEC can nearly double the required bandwidth for the signal [1], while ARQ can increase the network congestion that initially induced packet loss. However, unlike pure data, which must be received perfectly, visual data can be reconstructed using lossy signal processing techniques which exploit perceptual qualities and correlation within the image.

This paper addresses reconstruction of lost data in hierarchical subband coded images, in which subband decomposition is recursively performed on the low frequency subband. Subbands are assumed to be encoded and transmitted separately, allowing progressive transmission. Packet loss implies loss of coefficients whose locations within the received subbands are known to the receiver through use of packet sequence numbers and a predefined transmission order.

This work was supported by a National Science Foundation Graduate Fellowship and by IBM.

Because of their visual importance, edges play a primary role in defining the reconstruction algorithm. Incorrect reconstruction leads to blurring in synthesized edges, which is visually distracting. The subband decomposition provides a natural framework through which relationships between low and high frequency subbands can be used to characterize the low frequency signal for accurate edge reconstruction. Previous work on describing interband relationships has relied on heuristic techniques and additional processing of the low frequency band to relate activity in the low and high frequency signals. In [2], an empirically derived threshold measure is used to determine activity for each coefficient in the low frequency band, and this activity is used to predict the amplitudes of high frequency coefficients. In [3], an edge detector is applied to the low frequency band, the output of which is then thresholded. In both cases, the low frequency coefficients are used to determine edge structures and hence to select important high frequency coefficients. This paper presents a technique in which edge structures can be identified by examining high frequency subbands alone, without additional low frequency band processing. The edge identification is used to provide accurate low frequency edge reconstruction.

Two reconstruction techniques are presented, one for low frequency coefficients and one for high frequency coefficients. The low frequency algorithm exploits both intraband and interband correlations at the lowest level of subband decomposition to reconstruct coefficients in the visually important lowest frequency band (the LL-band). A smooth interpolative surface is fit to known data and the interpolation grid is then warped to maintain existing edge structures as determined by corresponding high frequency information (the LH- and HL-bands) at the same decomposition level. High frequency information is reconstructed using linear interpolation.

The organization of the paper is as follows. Section 2 presents a one dimensional edge model analysis for edge identification and classification. Section 3 describes low



1058-6393/95 $4.00 © 1995 IEEE

frequency reconstruction, and Section 4 presents high frequency reconstruction. Experimental results are detailed in Section 5. Section 6 summarizes and concludes the paper.

## 2. Edge Model Analysis

The visual quality of the reconstructed synthesized image is highly dependent on the quality of edge reconstruction, which is determined by the accurate reconstruction of low frequency coefficients in the vicinity of edges. Figure 1 illustrates one dimensionally the importance of edge placement. A simple edge model is defined as a 3-valued signal $(\ldots p_1, p_1, mp_1 + (1-m)p_2, p_2, p_2, \ldots)$, $0 < m \leq 1$. Analysis of this signal yields two different low frequency subband signals, depending on whether the subsampling occurs in even or odd locations. For the example shown using a 5-tap quadrature mirror filter (QMF) given in [2], the even-subsampled low frequency subband signal resembles a step function, while the odd-subsampled signal resembles a ramp. Reconstruction of the second coefficient in the step incorrectly as a ramp results in the synthesized edge placement offset by 1 pixel to the left from its correct location.

The high frequency subband contains edge information that can be used to characterize edge placement. The three-valued edge model is analyzed using a high-pass QMF derived from a low-pass QMF, for both even and odd length filters. The high frequency coefficients are functions of the edge parameter $m$ and the difference in pixel values across the edge $(p_1 - p_2)$. For a given filter, the behavior of the coefficients in the vicinity of edges can be therefore be characterized as a function of $m$, the subsampling pattern, and the coefficients' locations relative to the edge center. For both even and odd subsampling, regardless of the $m$ value, the two largest (in absolute value) high frequency coefficients are adjacent. Thus a simple edge can be detected by two adjacent large coefficients. These results hold regardless of filter length.

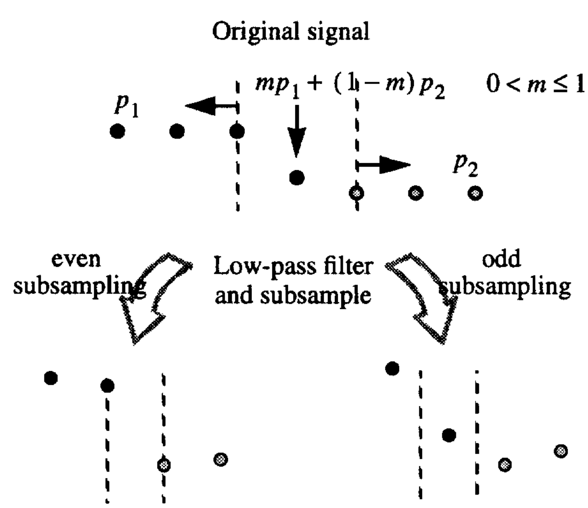


**Figure 1** A simple edge model and its low frequency subband as a function of the subsampling position. The edge center value is synthesized at the location between the dashed lines. Reconstruction of the second coefficient in either signal incorrectly results in a misplacement of the synthesized edge.

The *edge classification* for a single low frequency coefficient is determined by examining a window of five high frequency coefficients centered at the location of the lost low frequency coefficient, and looking for two adjacent large absolute values (the definition of "large" will be made more precise in Section 5). If there are zero, one, or two non-adjacent large coefficients, the edge classification is "normal," indicating that no edge is present. If there are two adjacent large coefficients, one of four patterns occur. If the pattern is $\{l\ l\ s\ s\ s\}$ or $\{s\ s\ s\ l\ l\}$ ($s$ referring to small and $l$ referring to large), then the lost coefficient is to the right or left of an edge, respectively. If the pattern is $\{s\ l\ l\ s\ s\}$ or $\{s\ s\ l\ l\ s\}$, then the coefficient is immediately on an edge or just beyond it, depending on the subsampling pattern. If there are more than two large coefficients occurring in any pattern, then the edge classification is "high frequency variations" (HFV), indicating that there is more high frequency activity than the simple edge model can predict.

Use of the edge model is easily extended to two dimensions for both vertical and horizontal edge classification in the LL-band by applying it independently in each direction. Because the LL-band contains a signal low-pass filtered and subsampled in both directions, the original properties of the signal are generally maintained following one dimensional analysis in either direction, and the edge model applies independently in both the horizontal and vertical directions. The LH-band at the lowest decomposition level contains the required high frequency information in the vertical direction to classify vertical edges, while the HL-band contains the corresponding information in the horizontal direction. The next section explains how horizontal and vertical edge classifications are used in reconstruction.

## 3. Edge Model Based Surface Generation for Low Frequency Reconstruction

### 3.1 Bicubic Interpolation

The high correlation present in the low frequency subband suggests that lost coefficients can be reconstructed using their neighbors, and the smooth, natural appearance of this subband suggests that interpolation should maintain this smoothness. Bicubic interpolation is selected as the surface generation technique, and is then modified to incorporate the edge information from the high frequency subbands. The bicubic surface can be considered to be a cubic spline surface with first order continuity on the edges. Requiring only first order continuity (that is, continuity in the first derivatives), is better suited to interpolation of low frequency subband coefficients than imposing higher order continuity constraints. First derivatives can

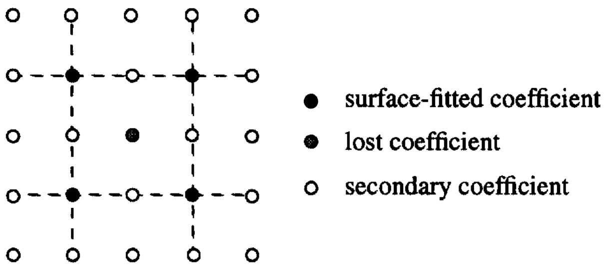


**Figure 2** Twenty-four coefficients used to reconstruct the lost value at the center. Surface-fitted values are used directly; secondary coefficients are used to estimate derivatives.

be reasonably estimated using differences of adjacent coefficients. Generation of higher order derivatives involves using more coefficients in a larger area, thus incorporating more global rather than local signal characteristics.

A cubic interpolating surface is fit to 4 known coefficients in the immediate vicinity of a lost coefficient using a total of 24 coefficients as illustrated in Figure 2. This surface exhibits local trends as defined by the data. While inclusion of the derivative terms provides some incorporation of the local surface structure, it is not enough to accurately place edges as discussed earlier. Hence the edge classification at the lowest decomposition level is used to warp the otherwise regular interpolation grid to better reconstruct the edges.

### 3.2 Grid Warping

One dimensional warping is conceptually understood as illustrated in Figure 3. First, a cubic polynomial is fit to two points and their derivatives on a regularly spaced grid, yielding an equation for the curve $\hat{f}(x)$. Interpolation of the center point on the grid gives $\hat{f}(1/2)$ and places the point approximately between the two end points. However, a warping of the grid to the left pushes the edge to the left and places a point closer to the rightmost value in the center. This is mathematically equivalent to interpolating the desired point as $\hat{f}(z), z > 1/2$, where the value of $z$ determines the extent of the warping. The curve can be similarly warped to the right by evaluating $\hat{f}(z), z < 1/2$.

Warping is determined by the edge classification based on a window of five high frequency coefficients centered on the location of the lost low frequency coefficient as discussed in Section 2. The edge classification indicates the location of the reconstructed coefficient with respect to the edge, but in practice, it is too difficult to select an individual interpolation point for each reconstructed coefficient. Therefore, the interpolation points are quantized to $(1/4, 1/2, 3/4)$ which roughly correspond to warping right (Figure 3(c)), center-based interpolation (Figure 3(a)), and warping left (Figure 3(b)), and an appropriate quantized interpolation point is selected.

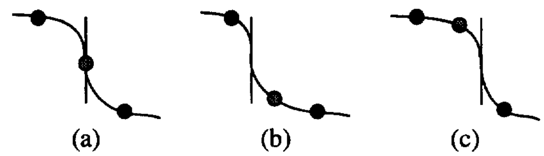


**Figure 3** Grid warping. The three curves have identical end points, but different center values. The interpolated value $\hat{f}(1/2)$ occurs on the vertical line in each edge, and in the center in (a). By pushing this value to the left, in (b), or to the right, in (c), the center value is biased toward the value on the right or left, respectively.

The quantized interpolation points for each edge classification are determined using a low-pass analysis of the edge model. Interpolation points as a function of the edge classification for odd-length filters are listed in Table 1. For the classes $\{l\,l\,s\,s\,s\}$, $\{s\,s\,s\,l\,l\}$, and $\{s\,l\,l\,s\,s\}$, the interpolation location is the same for both even and odd subsampling. However, for $\{s\,s\,l\,l\,s\}$, the location differs dependent on the subsampling pattern, and is a function of $m$. Therefore, more information is required than simply the edge classification. Referring to the two large coefficients in the high frequency signal as $l_{left}$ and $l_{right}$, this additional information is obtained by examining the ratio $l_{left}/l_{right}$, which is only a function of $m$ for any given filter. The ratio behavior is filter dependent and is characterized by plotting the function versus $m$ for each filter with even and odd subsampling. Interpolation points are then defined for various ranges of the ratio. Similar results can be determined for even-length filters. Warping is extended across two adjacent lost coefficients, with interpolation locations (1/6, 1/3, 1/2, 2/3, 5/6), and is also extended to two dimensions by applying it independently in the horizontal and vertical directions.

| Edge Classification | Low frequency reconstruction interpolation point |
|---|---|
| none | 1/2 |
| $\{l\,l\,s\,s\,s\}$ | 1/2 |
| $\{s\,l\,l\,s\,s\}$ | 3/4 |
| $\{s\,s\,l\,l\,s\}$ | $f(l_{left}/l_{right})$ |
| $\{s\,s\,s\,l\,l\}$ | 1/4 |
| >2 non-zero values | none* |

**Table 1** Low frequency interpolation point as a function of the thresholded high frequency signal. *Indicates high frequency variations.

### 3.3 Application to Low Frequency Reconstruction

The complete low frequency reconstruction algorithm is as follows. For each lost coefficient, the horizontal and vertical edge classifications are determined from the HL and LH-bands at the same decomposition level by thresholding the absolute values of the coefficients. Three scenarios can occur. In the first, neither class is high frequency variations. Then the interpolation locations are determined from the classifications, and derivatives are estimated using one- or two-sided differences. Unknown values that are required for calculation of either the four interpolation points or derivatives are estimated using weighted means, where unknown coefficients are estimated as the mean of available coefficients directly above, below, to the left, and to the right that are not classified as part of an edge structure based on their horizontal and vertical classifications. The lost coefficient is then generated using warped bicubic interpolation.

In the second scenario, the high frequency variations case is detected in only one direction. The lost coefficient is reconstructed following the procedure outlined above, but one-dimensional interpolation is performed in the direction with the non-HFV classification.

Finally, HFV can be detected in both directions. In this case, the threshold is increased until one direction has a non-HFV class and reconstruction proceeds as in the second scenario.

## 4. Linear Interpolation for High Frequency Reconstruction

Accurate reconstruction of the LH- and HL-bands at the lowest level of decomposition is important to assure accurate edge placement when reconstructing the low frequency band. Both the LH- and HL-bands exhibit high correlation only in the directions that have been low-pass filtered, and hence one-dimensional linear interpolation is performed in the low-pass direction. Unknown coefficients are interpolated from the two coefficients on either side of them in the low-pass direction (the Wiener-Hopf solution provides only a 0.5 dB improvement in SNR and no visual improvement). The HH band exhibits low correlation in both horizontal and vertical directions. Lost HH coefficients are not reconstructed; they are set to zero.

## 5. Experimental Results

Reconstruction begins at the lowest decomposition level with the LH-and HL-bands, which are in turn used to reconstruct the LL-band. Edge-model based surface generation is extended across any 2 adjacent lost coefficients, and individual coefficients are recursively reconstructed for greater loss. LH- and HL-bands in other decomposition levels are then reconstructed as they are received.

Algorithm performance was evaluated by reconstructing random loss of three coefficient groupings across all subbands at all decomposition levels: single coefficients, vectors of length 4, and blocks of size $2 \times 2$. In the case of length 4 vectors, the LH- and HL-bands were assumed vectorized in the high frequency direction to minimize the number of adjacent lost coefficients in the low frequency direction and hence improve the quality of reconstruction. USC database test images were subband decomposed to 1, 2, and 3 levels using various odd and even length quadrature mirror filters as given in [4], [5].

Simulations to determine the threshold for identification of large coefficients in the LH- and HL-bands yielded best results with a threshold of 2 for one decomposition level. Because the energy in the QMFs is $\sqrt{2}$, the threshold is increased by a factor of 2 for each decomposition level.

In general, the reconstructed LH- and HL-bands provide accurate information for edge placement. Low frequency reconstruction performs well on horizontal, vertical, and strong diagonal edges. Uni-directional high frequency patterns are maintained, and spatial masking tends to reduce the visual effects of errors in multidirectional patterns. Setting lost HH coefficients to zero produces negligible visual effects. The visual effects of errors in low frequency reconstruction change as the number of decomposition levels increases. At one decomposition level, errors in edge reconstruction are visible as small, sharp discontinuities in edges. At two and three levels, edge reconstruction errors are visible as slight or moderate blurring in the vicinity of an edge, caused by multiple levels of upsampling and filtering. A segment from a 4-band decomposition of *couple* suffering 10% random vector loss and reconstructed using the algorithm is shown in Figure 5.

Loss and reconstruction of individual coefficients produces images with slightly higher PSNRs than those coded with vectors, which in turn have slightly higher PSNRs than those coded with $2 \times 2$ blocks. Randomly lost coefficients are most likely to have the highest number of known coefficients required in interpolation present. Randomly lost vectors are only missing coefficients in one direction, while blocks require the most coefficient estimation for use in interpolation. A plot of PSNR versus percentage loss for three types of loss for both one and two decomposition levels is shown in Figure 4 for *couple*.

Quantization of the high frequency subbands at the lowest decomposition level affects the reconstruction quality of the LL subband. Quantization that is too coarse destroys the edge classification patterns used to identify edges. For one decomposition level, a bit allocation in the LH and HL bands that does not produce graininess provides adequate information for reconstruction. For two decomposition levels, a bit allocation that is slightly greater than is necessary to eliminate graininess is required for adequate reconstruction.

Computational overhead at the decoder is a function of the number of decompositions and the filter length. For a five tap symmetric filter (i.e. having three unique values), the decoder overhead per percentage of lost coefficients across all bands is 0.5% for one level of decomposition.

For longer or asymmetric filters and higher numbers of decomposition levels, these values decrease.

## 6. Summary

A decoder-based reconstruction algorithm for hierarchical subband-coded images using quadrature mirror filters has been developed. Interband relationships based on QMF properties were derived and used to accurately reconstruct edge structures in the visually-important lowest frequency band. Surface fitting using bicubic interpolation provides the smooth characteristics required of the lowest frequency band, and warping the interpolation grid provides a simple technique for placing the edges.

The algorithm is applicable to a variety of source coding coefficient groupings, e.g., pulse-code modulation, vector quantization, or small block-based transform coding, and is applicable to progressive transmission or multirate applications. By requiring only the lowest decomposition level for reconstruction of the lowest frequency band, the progressive transmission quality of hierarchical subband coding is preserved, and only one level of progression is lost. The high frequency bands from higher decomposition levels can then be reconstructed and used in refinement as they are received. Flexibility across both coding and transmission techniques, combined with the low computational complexity and good quality, makes the algorithm a strong candidate for applications in which reconstruction of hierarchical subband-coded data with minimal system changes is required.

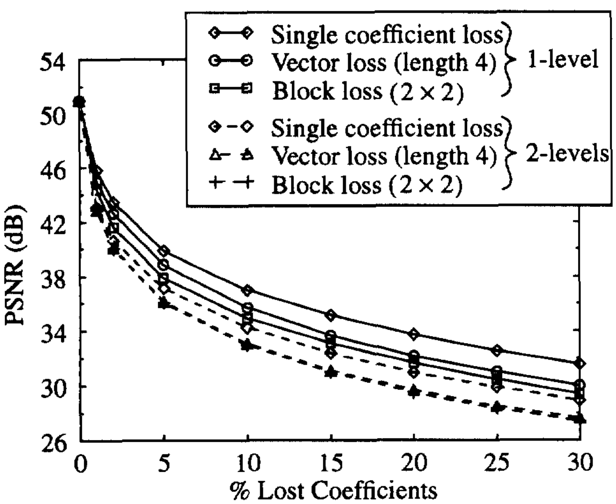


**Figure 4** Reconstruction performance on unquantized *couple* for one and two decomposition levels and random loss of isolated coefficients, 4-vectors, and $2 \times 2$ blocks.

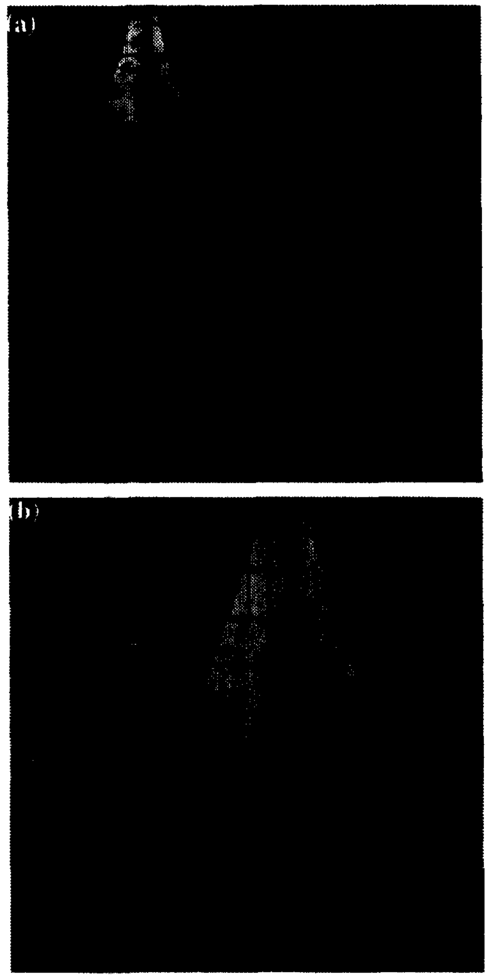


**Figure 5** Segment from *couple* (one decomposition level, 5-tap QMF) with 10% random vector loss in all subbands: (a) loss (b) reconstructed, PSNR = 34.1 dB.

## References

[1] N. Shacham & P. McKenney, "Packet Recovery in High-Speed Networks Using Coding and Buffer Management," *Proc. IEEE Infocom '90*, Vol. 1, pp. 124-31, San Francisco, CA, June 1990.

[2] O. Johnsen, O. V. Shentov, S. K. Mitra, "A Technique for the Efficient Coding of the Upper Bands in Subband Coding of Images," *Proc. ICASSP '90*, Vol. 4, pp. 2097-2100, April 1990.

[3] N. Mohsenian & N. M. Nasrabadi, "Edge-based Subband VQ Techniques for Images and Video," *IEEE Trans. Circuits and Systems for Video Technology*, Vol. 4, No. 1, pp. 53-67, Feb. 1994.

[4] J. W. Woods, *Subband Image Coding*, Chapter 4. Boston: Kluwer Academic Publishers, 1991.

[5] J. D. Johnston, "A Filter Family Designed for Use in Quadrature Mirror Filter Banks," *Proc. ICASSP '80*, Vol. 1, pp. 291-4, Denver, CO, April 1980.